J|A|C|S
COMMUNICATIONS

Published on Web 11/04/2008

Preparation of Hierarchical Hollow $CaCO_3$ Particles and the Application as Anticancer Drug Carrier

Wei Wei,[†] Guang-Hui Ma,*[,†] Gang Hu,[‡] Di Yu,[§] Tom Mcleish,[||] Zhi-Guo Su,[†] and Zhe-Yu Shen[†]

Institute of Process Engineering, Chinese Academy of Sciences, Beijing, 100190, PR China, Unilever Research China, Shanghai, 200233, PR China, Garvan Institute of Medical Research, Sydney, 2010, Australia, and School of Physics and Astronomy, Leeds University, LS2 9JT, U.K.

Received June 5, 2008; E-mail: ghma@home.ipe.ac.cn

An objective in materials science of increasing importance is to construct inorganic architectures with hierarchically complex structures and optimized properties, which have great potential as agents in optical, electronic, and magnetic applications.[1−5] Despite the various methods reported on the preparation of one-, two-, and three-dimensional crystal architectures, the organization of primary building units into hollow structures, though remaining a challenge for research activities on "crystal tectonics", still attracts much attention because of their promising applications in the encapsulation and controllable release of drugs, inks, flavors, and other chemical reagents.[6−8] So far, some hard template-assisted approaches have been demonstrated to be most effective for the preparation of hollow structures, which typically include the coating of nanocrystals on the surface of templates and the removal of the templates afterwards.[9−11] However, these methods tend to be rather complicated with an obvious drawback that the removal process often compromises the structural integrity of the final products and limits the practical applications.[12] Therefore, it is still highly desirable to develop a facile and mild method for the preparation of hollow structural devices.

$CaCO_3$ and products obtained from this compound are used in a wide range of fields. In addition to the conventional applications in toothpastes and cosmetics, in the paper industry, and in water treatment as a filtering material, this compound has also shown promising potential for the development of smart carriers for drugs.[13−19] Compared with many other inorganic materials previously used for similar purposes, $CaCO_3$ is exceedingly suitable because of its ideal biocompatibility and biodegradability properties.

Herein we describe a one-pot approach to couple the crystallization of $CaCO_3$ nanoparticles and the *in situ* symmetry-breaking assembly of these crystallites into hollow spherical shells under the templating effect of a soluble starch. Further investigation also reveals the desirable properties of these hierarchical particles (HPs) as anticancer drug carriers.

When very dilute solutions ($[Na_2CO_3] = 2.0$ mM; $[CaCl_2] = 2.0$ mM) were used, $CaCO_3$ spheres of ~500 nm in diameter were prepared at 30 °C (denoted as HP-a), as shown in Figure 1a. More detailed structural features are shown in Figure 1b, which makes it clear that the individual microspheres are hollow and composed of particulate building units of *ca.* 50 nm. The hollow structure is further revealed in the TEM image (Figure 1c) showing clearly the stacking of the building units (shown in the inset) and the interior cavity of the sphere since the contrast at the center is much lower than that of a solid particle (Figure S7c). Other detailed characterizations are available in Figures S1, S2, and S3.

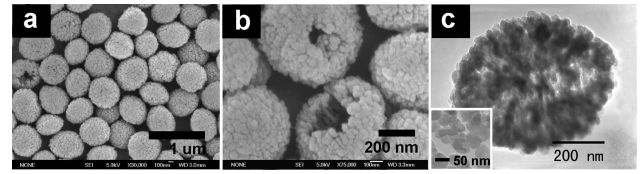

Figure 1. $CaCO_3$ superstructures synthesized at 30 °C. SEM images showing (a) the uniform particle size of the spheres and (b) some defects on the surface indicating the hollow structure of the spheres. (c) TEM image of a single sphere with low contrast at the center with an inset high-resolution TEM image of the primary building units.

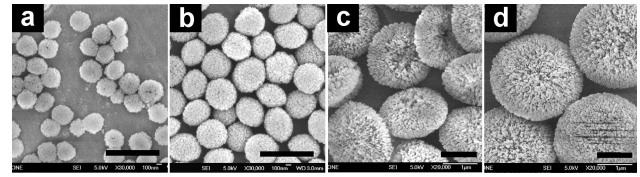

Figure 2. SEM images of $CaCO_3$ superstructures of different size prepared at different temperatures of (a) 15, (b) 30, (c) 50, and (d) 70 °C (scale bar: 1 μm).

Meanwhile, we also noticed that the particle size of HP-a was highly dependant on the reaction temperature. The reaction was tried at different temperatures, and the HP-a grew bigger from *ca.* 300 nm at 15 °C, 500 nm at 30 °C, 2 μm at 50 °C, to 2.5 μm at 70 °C (Figure 2). The higher the reaction temperature, the more developed a structure the spheres have. Such a tendency is revealed by two TEM images shown in Figures 1c and S4a with the latter showing an obvious low contrast at the core indicating a more developed wall structure around. A cross-sectional image (Figure S4b) provides direct evidence of this feature and reveals that such spherical superstructures are constructed through a hierarchical self-assembly process which includes the assembly of primary particulate building units (Figure S4c inset) into fibrous secondary ones followed by the assembly of the secondary fibrous ones into the spherical shells.

Similar structures were obtained by Mann et al. in their study on $CaCO_3$ and some metal oxides.[20,21] The authors proposed that such structures could be induced by a progressive dissolution of the initial metastable phase in the initially spherical structures, a redistribution of matter afterwards from the interior to exterior of the microspheres, and the recrystallization of more stable polymorphs in the reaction system. In the present study, a series of intermediates were also trapped, listed in Figure 3, which clearly reveal that the formation of these hollow HP-a went via a ring-like structure (Figure 3a and 3b) at the early stage. The particulate primary building blocks can be discerned from the image, but the fibrous secondary units are not well-developed. With the reaction going on, the rings are getting thicker to form a doughnut-like

[†] Chinese Academy of Sciences.
[‡] Unilever Research China.
[§] Garvan Institute of Medical Research.
[||] Leeds University.

 10.1021/ja8039585 CCC: $40.75

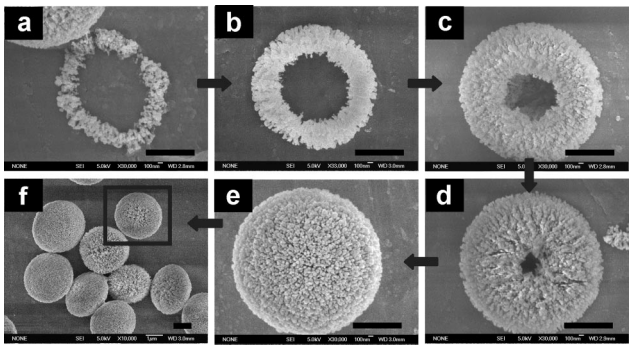

Figure 3. SEM images of a series of intermediates trapped during the synthesis of HP-a at 70 °C, indicating the morphological growth of the $CaCO_3$ shells (scale bar: 1 μm).

structure (Figure 3c) until the voids are closed, to form a rounded shell (Figure 3d to e). It is very clear that the crystallization of the primary building blocks and the self-assembly of these particulates into higher-order structures occurred simultaneously. This phenomenon is obviously different from the structural evolution described by Mann et al. mentioned above. Although we found it difficult to trap any form more immature than the ring-like structure shown in Figure 3a due to the very speedy growth of these structures, it has been very clear that the formation of hollow spheres results from the crystallization of nanoparticles coupled with a simultaneous multiscale assembly. We believe the key point in understanding the mechanism of the present study should be focused on the formation of the ring-like structure in Figure 3a and on any prior phase if possible. An *in situ* observation of the whole reaction should reveal more information of the crystallization process, and relevant work is in progress.

Furthermore, we also observed that the products underwent a phase evolution as well as a morphology change when more concentrated solutions were tried (Figures S5−S9). We propose that the crystallization of $CaCO_3$ was modified by the starch templates, which undergo a conformational transition on their helices when interacting with calcium cations in the solution. The degree and nature of complexation of the starch with the growing crystal depend on the ionic strength, and as a consequence, $CaCO_3$ superstructures of different structural features were induced with the template effect of the starch. Though it is so far still unclear how the starch template interacts with the $CaCO_3$ crystallites all through the reaction, the study using IR and CD still gives very informative indications of the interaction between starch and $CaCO_3$ and the structural transition of the starch used at different reaction conditions (Figures S10 and S11). In particular, the more exotic self-assembled hollow-sphere structures (HP-a) contain the greatest amount of starch in the final assembly (Figure S12). Two features of the implicit templating process indicate a very subtle interaction between the two components: (1) the delicate balance of the concentrations of polymeric starch and crystallisable solute; (2) the extraordinary symmetry-breaking of the early stages of self-assembly into the transient ring-structure. One possible underlying process invokes couplings between the local crystal forms and geometries of the $CaCO_3$ aggregates and the starch complexed to it, together with a second coupling between the local starch concentration and the local flux of solute onto the growing crystal or aggregate. As a result of these nonlinear couplings of structure and fluxes, symmetric growth may become unstable and give way to spherulitic/cone forms (in 3D) or ring forms (in 2D). The aggregation rates become self-sustainingly higher on the cone base (or exterior of the ring). In the mature stages an entire shell is formed, providing that the initial symmetry breaking occurs gently

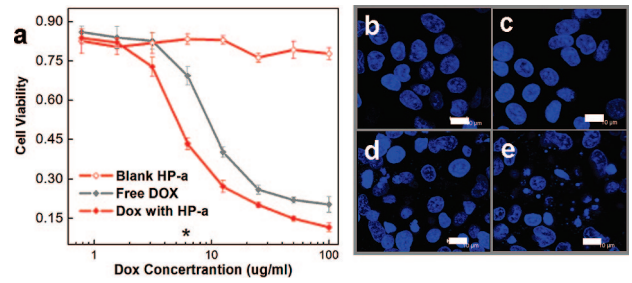

Figure 4. (a) Cytotoxicity of HepG2 cells exposed to free DOX, blank HP-a, and DOX loaded HP-a for 48 h (Mean ± SD, $n = 4$). The right panel showing the nuclei of original HepG2 cells (b) and the HepG2 cells incubated with blank HP-a (c), free DOX (d), and DOX loaded HP-a (e) after 48 h. The concentrations of additives were corresponding to the star-marked point in (a) (scale bar: 10 μm).

enough and the accretion of fibrils onto the ring is faster than accretion to its interior. Exploration of this hypothesis will require a more detailed knowledge of the spatial disposition of the starch and its coupling to ionic fluxes.

In the past several years, cancer therapy based on new drug carriers, such as microcapsules, nanotubes, and hollow nanoparticles, has arisen as a promising research area.[22−24] Although those established methods allow drugs to be delivered to specific lesion sites, they face the difficulty of preventing the leakage of drugs before arriving at the target location, which may also lead to side effects and reduce the bioavailability.[25] An ideal regime will respond to the intracellular environment and release the carried drug directly to the cancer cell. Herein, HP-a has such an attractive property since the component $CaCO_3$ rends the system only triggered by the extracellular acid environment in solid tumor tissues (pH = 6)[26] or lysosomes inside cancer cells (pH = 4.5).[27] Compared to a conventional synthesized pH-sensitive platform, this device also has a high biocompatibility due to the component $CaCO_3$, which is necessary for the clinical application.

The anticancer drug doxorubicin (DOX) was loaded on the HP-a (prepared at 30 °C) to test the feasibly of such a device for anticancer therapy. As shown in Figure S14a, The release of DOX from HP-a was almost undetectable for over 48 h under physiological conditions (pH = 7.0−7.5). In contrast, the DOX release gradually increased around pH 6.0 and 5.0, suggesting a good response to the pH values in extracellular sites in tumor tissues and lysosomes in cancer cells, respectively. We also took advantage of the autofluorescence of DOX to observe its release from HP-a and found a dramatic decrease of the autofluorescence in a low pH value environment (Figure S14b−d), indicating more release in response to the acidity. We further evaluated HP-a as a pH-sensitive drug carrier *ex vivo*. The structure could be well maintained when HP-a were only incubated in the cell culture medium containing 10% serum (Figure S15b). However, HP-a extracted from HepG2 cells at 48 h after the uptake showed obvious deconstruction (Figure S15a). These results confirmed the favorable stability of HP-a in the plasma before arriving at the target site and the satisfied pH response to the acid environment in the tumor tissues and lysosomes.

The effects of DOX carried by HP-a on liver carcinoma HepG2 cells were examined afterwards. As shown in Figure 4a, HP-a alone showed almost no cytotoxicity to HepG2 cells, indicating its good biocompatibility. However, once loaded with DOX, HP-a greatly increased the death of HepG2 cells over the effect of DOX by itself. It was also confirmed by the morphological change of nuclei observed by CLSM (Figure 4b−e). 48 h after treatment, cells with unloaded HP-a showed normal morphology of nuclei as untreated

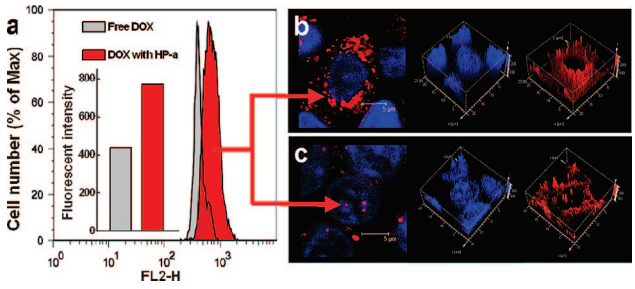

Figure 5. (a) HepG2 cell uptake of free DOX and DOX loaded HP-a. Perinuclear accumulation (b) and nuclear location (c) of DOX loaded HP-a (red dot). The experiments were performed at 6 h after incubating HepG2 cells with DOX or DOX loaded HP-a, at the concentration corresponding to the star-marked point in Figure 4a (scale bar: 5 μm).

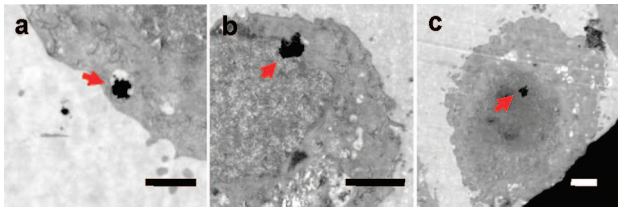

Figure 6. TEM images of HP-a (indicated by red arrow) uptake by HepG2 cells. The HP-a was first phagocytosed into vesicle (a), localized around nucleus afterwards (b), and finally intruded into the nucleus (c) (scale bar: 1 μm).

cells. On the contrary, nuclear fragmentation and condensation were revealed in most of the cells treated with DOX loaded HP-a, while only a few condensed nuclei presented in the cells treated with the DOX solution (see the corresponding DNA ladder analysis in Figure S16).

To investigate the mechanism of the higher cytotoxicity induced by DOX loaded HP-a, the amount of DOX uptake into HepG2 cells was monitored via DOX-derived fluorescence by a flow cytometer 6 h after treatment, as the star-marked point in Figure 4a. As shown in Figure 5a, the cellular fluorescence is much higher when the DOX was loaded on HP-a, which indicates that HP-a, as a drug carrier, enhances the cell uptake of DOX.

Most cancer chemotherapy drugs, including doxorubicin, interact with nuclear DNA to cause DNA damage and topoisomerase inhibition and, consequently, stop the process of replication and induce cell death.[28−30] Unfortunately, cancer cells have developed several mechanisms to limit the access of anticancer drugs to cell nuclei, which is one of the major reasons for the resistance of tumor cells to anticancer drugs.[31,32] To our surprise, after being taken in the cell, the HP-a carrier could aggregate around the nucleus and even directly intrude into the nucleus (CLSM images in Figure 5 and TEM images in Figure 6). Referring to some previous reports,[33] we proposed that the phenomenon might be attributed to the electrostatic interaction between the negatively charged nucleus and the positively charged DOX-loaded $CaCO_3$ particles (z potential = 5.8 mV). In addition to the increased uptake, these behaviors would obviously enhance the nuclear delivery efficiency for anticancer drugs, and consequently better tumor cytotoxicity would be achieved.

In summary, we have proposed a facile method to prepare hollow $CaCO_3$ particles HP-a, formed by the self-organization of nanocrystallites. The formation process and hierarchical structure are also investigated. Further functional study using HP-a as an anticancer drug carrier for DOX demonstrates its advantages for localizing drug release by the pH value-sensitive structure and enhancing cytotoxicity by increasing cellular uptake, perinuclear accumulation, and nuclear entry.

Acknowledgment. This work was supported by the National Nature Science Foundation of China (20536050, 20221603 and 20636010), Chinese Academy of Sciences (KJCX2-YW-M02), and the Knowledge Innovation Program.

Supporting Information Available: Experimental Section, HP-a characterizations, SEM and TEM images, XRD data, CD measurement, IR spectra, TG analysis, and DNA ladder. These materials are free of charge via the internet at http://pubs.acs.org.

References

(1) Pacholski, C.; Kornowski, A.; Weller, H. *Angew. Chem.* **2002**, *41*, 1188.
(2) Goldberger, J.; He, R.; Zhang, Y.; Lee, S.; Yan, H.; Choi, H. J.; Yang, P. *Nature* **2003**, *422*, 599.
(3) Bowden, N.; Terfort, A.; Carbeck, J.; Whitesides, G. M. *Science* **1997**, *276*, 233.
(4) Gracias, D. H.; Tien, J.; Breen, T. L.; Hsu, C.; Whitesides, G. M. *Science* **2000**, *289*, 1170.
(5) Whitesides, G. M.; Grzybowski, B. *Science* **2002**, *295*, 2418.
(6) Lee, Y.; Lee, J.; Bae, C. J.; Park, J. G.; Noh, H. J.; Park, J. H.; Hyeon, T. *Adv. Funct. Mater.* **2005**, *15*, 503.
(7) Han, S.; Jang, B.; Oh, S. M.; Hyeon, T. *Adv. Funct. Mater.* **2005**, *15*, 1845.
(8) Caruso, F.; Caruso, R. A.; Mohwald, H. *Science* **1998**, *282*, 1111.
(9) Yin, Y.; Lu, Y.; Gates, B.; Xia, Y. *J. Am. Chem. Soc.* **2001**, *123*, 8718.
(10) Sun, X.; Liu, J.; Li, Y. *Chemistry* **2006**, *12*, 2039.
(11) Nakashima, T.; Kimizuka, N. *J. Am. Chem. Soc.* **2003**, *125*, 6386.
(12) Yu, H.; Yu, J.; Liu, S.; Mann, S. *Chem. Mater.* **2007**, *19*, 4327.
(13) Saleem, I. Y.; Vordermeier, M.; Barralet, J. E.; Coombes, A. G. *J. Controlled Release* **2005**, *102*, 551.
(14) Ikoma, T.; Tonegawa, T.; Watanaba, H.; Chen, G.; Tanaka, J.; Mizushima, Y. *J. Nanosci. Nanotechnol.* **2007**, *7*, 822.
(15) Lucas-Girot, A.; Verdier, M. C.; Tribut, O.; Sangleboeuf, J. C.; Allain, H.; Oudadesse, H. *J. Biomed. Mater. Res. B: Appl. Biomater.* **2005**, *73*, 164.
(16) Ueno, Y.; Futagawa, H.; Takagi, Y.; Ueno, A.; Mizushima, Y. *J. Controlled Release* **2005**, *103*, 93.
(17) Zhao, Y.; Carvajal, M. T.; Won, Y. Y.; Harris, M. T. *Langmuir* **2007**, *23*, 12489.
(18) Lynch, R. J.; Cate, J. M. *Int. Dent. J.* **2005**, *55*, 175.
(19) Pickles, M. J.; Evans, M.; Philpotts, C. J.; Joiner, A.; Lynch, R. J.; Noel, N.; Laucello, M. *Int. Dent. J.* **2005**, *55*, 197.
(20) Yu, J. G.; Guo, H. T.; Davis, S. A.; Mann, S. *Adv. Funct. Mater.* **2006**, *16*, 2035.
(21) Yu, J. J.; Yu, H. G.; Guo, H. T.; Li, M.; Mann, S. *Small* **2008**, *4*, 87.
(22) Meng, F. T.; Ma, G. H.; Qiu, W.; Su, Z. G. *J. Controlled Release* **2003**, *91*, 407.
(23) Wang, L. Y.; Ma, G. H.; Su, Z. G. *J. Controlled Release* **2005**, *106*, 62.
(24) Ali-Boucetta, H.; Al-Jamal, K. T.; McCarthy, D.; Prato, M.; Bianco, A.; Kostarelos, K. *Chem. Commun. (Camb)* **2008**, 459.
(25) Ganta, S.; Devalapally, H.; Shahiwala, A.; Amiji, M. *J. Controlled Release* **2008**, *126*, 187.
(26) Helmlinger, G.; Yuan, F.; Dellian, M.; Jain, R. K. *Nat. Med.* **1997**, *3*, 177.
(27) Bae, Y.; Fukushima, S.; Harada, A.; Kataoka, K. *Angew. Chem.* **2003**, *42*, 4640.
(28) Fuertes, M. A.; Castilla, J.; Alonso, C.; Perez, J. M. *Curr. Med. Chem. Anticancer Agents* **2002**, *2*, 539.
(29) Pommier, Y. *Nat. Rev. Cancer* **2006**, *6*, 789.
(30) Quintas-Cardama, A.; Kantarjian, H.; O'Brien, S.; Jabbour, E.; Giles, F.; Ravandi, F.; Faderl, S.; Pierce, S.; Shan, J.; Verstovsek, S.; Cortes, J. *Cancer* **2006**, *107*, 1525.
(31) Gottesman, M. M.; Fojo, T.; Bates, S. E. *Nat. Rev. Cancer* **2002**, *2*, 48.
(32) Mathieu, A.; Remmelink, M.; D'Haene, N.; Penant, S.; Gaussin, J. F.; Ginckel, R. Van; Darro, F.; Kiss, R.; Salmon, I. *Cancer* **2004**, *101*, 1908.
(33) Xu, P.; Van Kirk, E. A.; Zhan, Y.; Murdoch, W. J.; Radosz, M.; Shen, Y. *Angew. Chem., Int. Ed.* **2007**, *46*, 1.

JA8039585